Analysis of neoclassical tearing mode stabilization experiment by electron cyclotron injection in KSTAR

MinSooCha[1], MinHo Woo[2], SangheeHahn[2], YoungSeokPark[2], Minjun J Choi[2], Jong-Kyu Park[1], Byoungho Park[2], AndrewRothstein[3], EgemenKolemen[3,4], and Yong-SuNa[1*]

[1]Department of Energy Systems Engineering, Seoul National University, Seoul, Korea
[2]Korea Institute of Fusion Energy, Daejeon, Korea
[3]Department of Mechanical and Aerospace Engineering, Princeton University, Princeton, New Jersey, United States of America
[4]Princeton Plasma Physics Laboratory, Princeton, New Jersey, United States of America

Abstract . We report the neoclassical tearing mode (NTM) stabilization experimental results by injection of the electron cyclotron (EC) beam in KSTAR, and its analysis with integrated modelling. In the KSTAR experiment, NTM was intentionally induced and the EC beam was injected by the plasma control system (PCS) to stabilize it. Here, the EC angle was controlled based on the minimum seeking algorithm for the island growth rate. Although the EC angle was not changed significantly, the island width significantly decreased towards the end of the experiment followed by the recovery of plasma pressure. To assess the NTM stabilization experiment from a stability perspective, we performed integrated modelling with TRIASSIC utilizing the reconstructed equilibrium with magnetic diagnostics and motional stark effect diagnostics. As a result, we observed that the NTM is stabilized by EC

1 Introduction

Neoclassical tearing mode (NTM) is a resistive magnetohydrodynamic (RMHD) instability that destabilizes a magnetic island in magnetized plasma. It has can significantly degrade confinement of a fusion plasma by enhancing transport and may even lead to plasma disruptions [1,2]. The poloidal/toroidal mode number m/n = 2/1 NTM damages plasma performance more than NTMs with mode numbers of 3/2 or higher [3]. NTMs are characterized by the loss of bootstrap current due to the flattened pressure profile within magnetic islands, which can make the NTM more unstable. Therefore, avoiding or stabilizing of NTMs is necessary to achieve stable operation of high-performance plasma for nuclear fusion.

The NTMs can be stabilized by adjusting current drive by compensating the missing bootstrap current [4]. Electron cyclotron (EC) beam injection is a promising strategy for stabilizing NTMs by current drive (ECCD) and heating (ECH). However, if the ECCD deposition is not aligned well to the island O-point, it may even destabilize it [5]. Therefore, it is important to align the EC to the location of the island accurately. Various control algorithms have been utilized for this purpose [6]. For instance, the search and suppress algorithm finds the location of NTM by scanning the EC deposition, then locks it. The target lock algorithm sweeps and jitters the EC deposition to construct a probability potential function from the time-series data, offering faster stabilization than the search and suppress algorithm but being more sensitive to noise. The active tracking algorithm tracks the NTM based on diagnostics. The minimum seeking algorithm [7-9] perturbs the EC deposition and monitors the response of plasma, to identify a local minimum, where the NTM can be stabilized. Such techniques have been used in tokamaks including DIII-D [10], ASDEX Upgrade [11], TEXTOR [12], Tore Supra [13], TCV [14], KSTAR [15], and JT-60U [16]. Among these algorithms, the minimum seeking method can overcome the resolution issues of diagnostics despite the considerable developments since it needs to diagnose the island width only by assuming the island width (or its growth rate) is a function of the EC angle. It has the advantage that can track the NTM after searching its location, but less robust to gain values that determining the perturbation of the EC angle. The minimum seeking algorithm is particularly simple when multiple EC launchers can be mapped to same deposition. Their toroidal spacing in a same poloidal plane enables this, allowing us to monitor WKH LVODQG ZLGWK ¶V UHVSRQVH WR requiring complex calibrations. Also, several numerical studies have suggested that using the island width growth rate rather than the island width itself is more efficient when employing the minimum seeking algorithm [17-19]. When the controller tries to reduce the island width growth rate, it may find the path to reduce island width and its growth rate simultaneously, while the growth rate can increase if the controller uses island width itself.

The stability of the NTM can be analysed by calculating ûZKLFK is a stability index for a tearing mode [20]. This index is directly related to the growth of tearing

* Corresponding author: ysna@snu.ac.kr

mode [21] and is contained in modified Rutherford equation (MRE) [10,22]. We can calculate the evolution of the island width of the tearing mode with the MRE. In this paper, we analysed the NTM stabilization experiment that utilized the feedback control of EC by minimum seeking method for the island width growth rate. The remainder of this paper is organized as follows. In section 2, the result of the KSTAR experiment utilizing the minimum seeking algorithm with EC to suppress the NTM is examined. In section 3, we analyse the stability of NTM in this experiment with the integrated modelling using TRIASSIC [23] with a simplified MRE [24]. Finally, the findings will be summarized in section 4.

2 Experimental results

2.1 Feedback control algorithm

We had implemented the EC controller based on the minimum seeking algorithm with island width growth rate in the KSTAR plasma control system (PCS). The controller employs a boxcar operation to average the n = 1 mode amplitude in order not to consider noise or rapid plasma perturbations. Several numerical studies using minimum seeking algorithm for tearing mode control assumed perfect alignment at the beginning of the simulations. However, for experimental application, the implemented controller adopts an additional scan phase for the alignment before applying minimum seeking algorithm. Firstly, in the scan control phase, the controller scans EC poloidal angle to find where the NTM is, by evaluating the growth rate of the averaged n = 1 mode amplitude. If the location of NTM is identified, the controller tracks it by perturbing the poloidal angle. The adjustment of the angle is determined using the finite difference method. The perturbations of poloidal crank angle used in scan and precise in control is determined as following equations,

$$\Delta\theta_{scan} = K_{scan} \quad (1)$$

$$\Delta\theta_{precise} = K_{precise}\,\Delta\dot{W}\ sign(dt/d\theta) \quad (2)$$

Where $\Delta\theta$ and K are perturbation and gains, respectively, for scan and precise control phase denoted by subscripts.

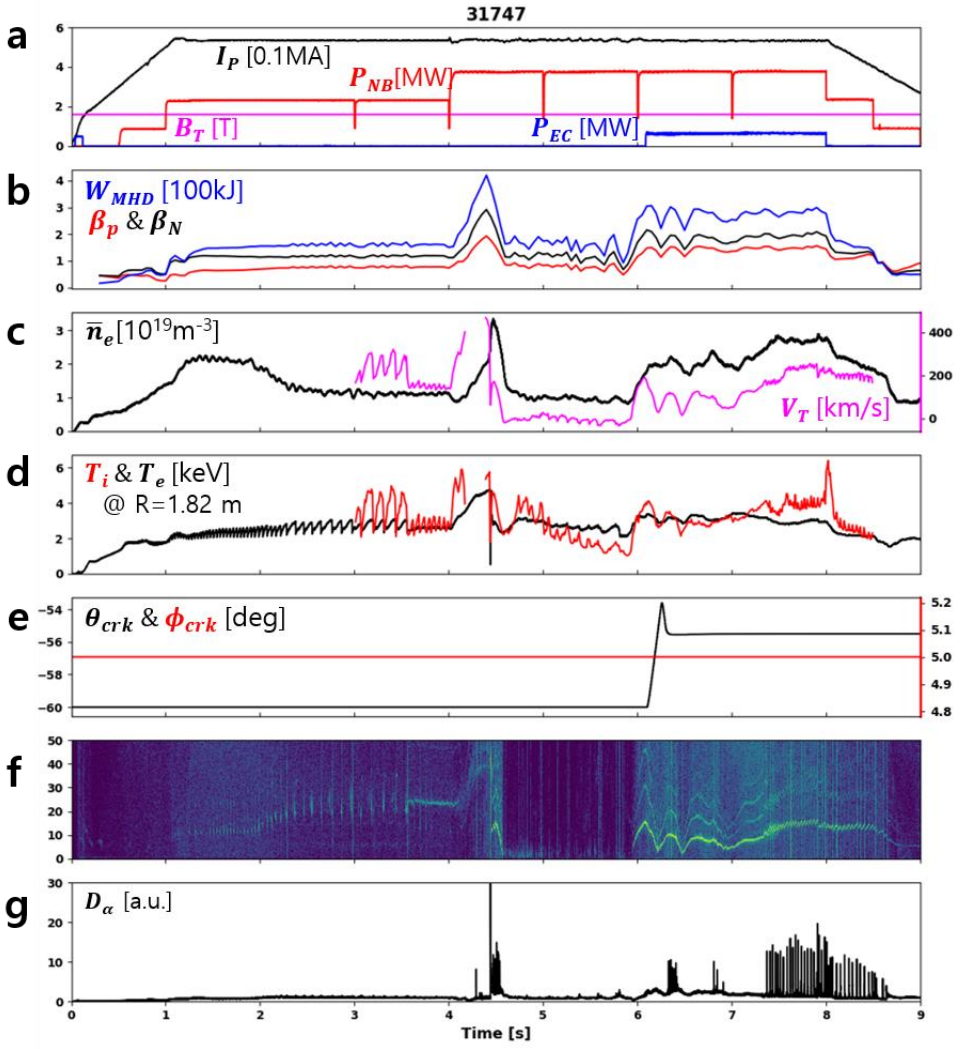

Fig. 1. Time evolution of main parameters in the NTM stabilization experiment, KSTAR shot #31747. **a.** The plasma current (I_P), toroidal magnetic field (B_T) at the magnetic axis, and NB and EC injection power (P_{NB} and P_{EC}). **b.** The stored plasma energy (W_{MHD}), plasma normalized beta (β_N), and poloidal beta (β_p). **c.** The electron line-averaged density ($\bar{n}_e$) and central toroidal rotation velocity (V_T). **d.** The central ion and electron temperature (T_i and T_e). **e.** EC poloidal and toroidal crank angle (θ_{crk} and ϕ_{crk}). **f.** The magnetic fluctuation by Mirnov coils. **g.** The D_α emission intensity.

$\Delta\dot{W}$ is difference of the island width growth rate. The reason for the controller perturbs the EC deposition after scanning is that the assumed function might change due to variations in plasma conditions or EC injection. In the KSTAR 2022 experiment, we utilized this controller to stabilize a 2/1 NTM.

2.2 Stabilization of n = 1 mode

In KSTAR shot #31747, we intentionally lowered the toroidal magnetic field compared to the conventional KSTAR experiments to inject EC near the typical location of the 2/1 NTM. The plasma current was set to be 530 kA. We injected total 3.7 MW of neutral beams (NBs) and 0.5, 0.7 MW of ECs for the plasma start-up and the NTM control by PCS, respectively. The selection of control algorithm leads us to use several EC launchers but it is our next scope. The experimental results are summarized in fig. 1. The plasma was diverted at 4.0 s, with the additional two of NB injections. As a result, the plasma performance was rapidly improved and a n = 1 instability appeared after 4.44 s. This mode seems to interact with the eddy currents flowing in the plasma wall, leading to a decrease in plasma rotation and the plasma was finally locked. At 5.94 s, the locking was spontaneously released without any additional control and the plasma started rotating again that PCS can detect the n = 1 mode amplitude. Then the PCS injected EC based on the minimum seeking algorithm. The detailed illustration of the EC angle and mode amplitude can be found in fig. 2. The PCS began controlling EC angle and actual injection at 6.09 s. The scan control was ended at 6.26 s then the precise control was acted until 8.0 s.
There are two limitations in this experiment, firstly, the minimum seeking controller needs saturated NTM but the fluctuation of the mode leads misjudgment of the NTM location. Secondly, the EC angle perturbation in the precise control phase is quite small since the gain value was setted too small. We will address these limitations to see the clear feedback control with further experiment. The plasma fluctuated immediately after the release of locking, and the fluctuation became stable after 6.7 s and the amplitude of the n = 1 mode was diminished, implying it has been stabilized. As a result, improvement in the plasma confinement factor, β_p, and toroidal rotation were observed.

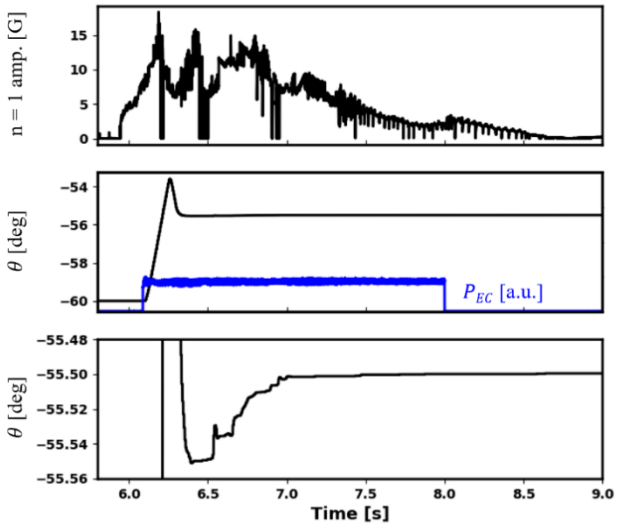

Fig. 2. a. Mode amplitude of n = 1 instability. b. The controlled EC angle and injected EC power of 700 kW. Enlarged image of controlled EC angle.

2.3 Identification of n = 1 mode

To determine what the n = 1 mode is, we need to find poloidal mode number and its characteristics. While n can be easily obtained with a toroidal Mirnov coil set, it is hard to identify the poloidal mode number, m. Despite the challenge, we aimed to identify the rough poloidal structure, by examining how the phase of the magnetic perturbations induced by the instability varies with the position of the poloidal Mirnov coil. We band-pass filtered a set of poloidal Mirnov coil data with the rotation frequency of the n = 1 mode and arranged according to the poloidal angle of each coil. With this procedure, we isolated the magnetic perturbation waveform caused by the n = 1 instability. In fig.3, the n = 1 mode rotating with 14.5 kHz at 7.75 s is repeated two times poloidally, so once can figure out it is 2/1 mode.

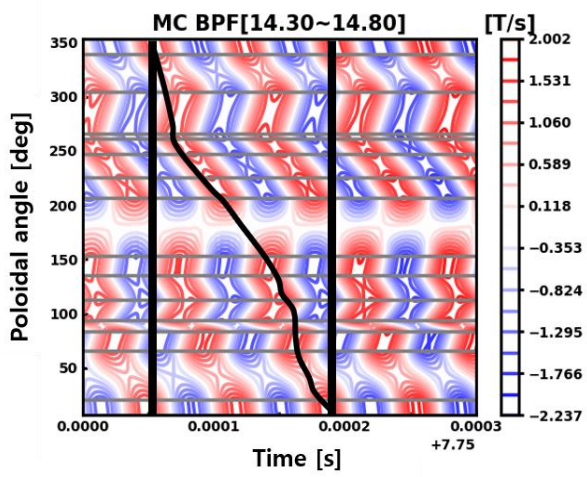

Fig. 3. Set of band-pass filtered poloidal Mirnov coil data in KSTAR shot #31747.

To classify whether the 2/1 mode is a tearing or a kink mode, there is a need to find whether the mode induced phase inversion. In the case of the tearing mode, the plasma pressure is flattened within island so that its poloidal rotation leads to the phase inversion that can be detected by electron cyclotron emission (ECE) or soft X-ray diagnostics. The ECE image installed in KSTAR [25] allows for the diagnosis of electron temperature fluctuations in 24 × 8 channels with 1-2 cm spatial and 0.5-2 [illegible] As a result, we could get a V spatial structure and temporal advances of the normalized fluctuation $dT_e/\langle T_e \rangle$, where dT_e is the electron temperature fluctuation and $\langle T_e \rangle$ is overall level of T_e. In fig.4.a, an outflow of T_e towards the plasma edge in upper left of the image is observed. As the 2/1 instability rotates, an inflow is observed in fig.4.b. This phase inversion confirms that the 2/1 instability is

indeed a 2/1 tearing mode. In detail, Fig.4.a and fig.4.c correspond to the O-point and X-point, respectively, while fig.4.b shows the intermediate phase. The ECEI results shows the flattening of the electron temperature profile that would lead to a decrease of the bootstrap current, implying the 2/1 tearing mode is neoclassically driving. Based on these mode analyses, we conclude the nature of n = 1 instability is a 2/1 NTM.

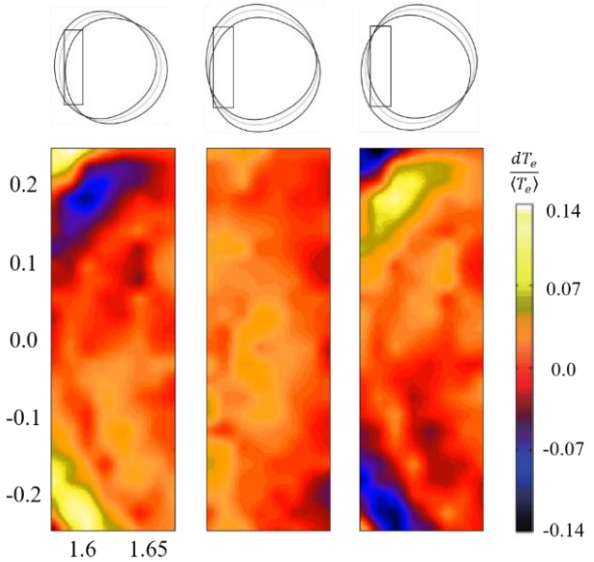

Fig. 4. ECE images of 2/1 instability in KSTAR Shot#31747 at R~1.6m and its corresponding location of magnetic island.

2.4 Alignment results of EC with NTM

To analyse the alignment between EC and NTM in this experiment, we used TORAY code [26] to model the ECCD and ECH profiles provided by motional stark effect (MSE) constrained equilibrium with the EFIT code [27,28]. Fig.5.a illustrates the mode amplitude and β_p in black and blue, respectively. Fig. 5.b shows the location of NTM (r_s) in red line, and the green line shows the peak of the ECCD profile (r_{ec}) and its full-width half maximum (FWHM, δ_{ec}) with the green shaded area. Before 7.3 s, the plasma is highly fluctuating and the amplitude of NTM and β_p varying concurrently despite the EC injection. After 7.3 s, the alignment appears to be effective, leading to the cessation of the observed behaviours. During this period β_p increases while the amplitude of the NTM decreases, supported by normalized misalignment $\frac{|r_{ec}-r_s|}{\delta_{ec}}$ being less than 0.5, as in fig.5.c. Therefore, it is thought that the alignment of the EC deposition has a stabilizing effect to the 2/1 NTM, resulting in improved plasma performance.

3 Stability analysis

To identify which mechanism stabilized the 2/1 NTM dominantly, we computed each term of simplified MRE [24] with integrated modelling using TRIASSIC. The simplified MRE computes the growth rate of the magnetic island with various effects such as the classical tearing index, its correction considering the local perturbation of the current profile by ECCD, the destabilizing effect of bootstrap current, small island and polarization threshold stabilizing term, and effect of ECCD/ECH. To obtain plasma parameters such as the temperature, safety factor profile, and bootstrap current density contained in the simplified MRE, we constructed an equilibrium constrained by magnetic, MSE diagnostics, and plasma pressure profiles. The time series values of these parameters are computed by the simulation using TRIASSIC. In this simulation, we used CHEASE [29] to solve Grad-Shafranov equation, NUBEAM [30] and TORAY to model the NB and EC injection, respectively. The bootstrap current profile is computed with the Sauter model [31]. We computed the each MRE terms with the acquired plasma parameters. Fig.5.a illustrates the normalized island width growth according to the island width in the 7.75 s of the experiment. We could easily find that ECCD related terms, denoted by orange and purple lines, have stabilizing effects at any width, while ECH exhibits little effect. Fig.5.b presents the values of the MRE terms in experimental time domain. Since the simulation began with the experimental results when the plasma

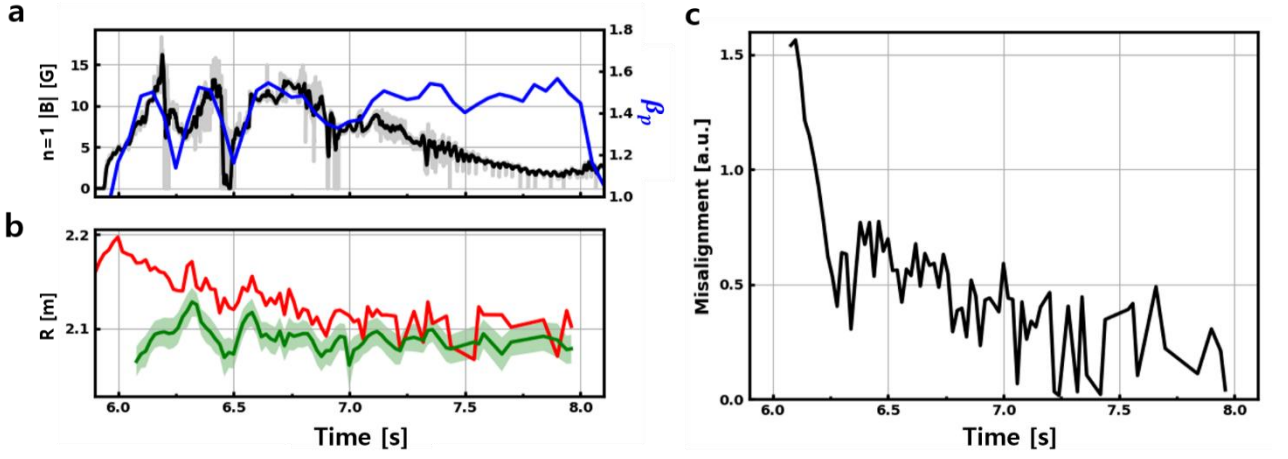

Fig. 5. Time evolution of main parameters regarding NTM stabilization. a. The amplitude of 2/1 NTM amplitude (black) and (blue). b. The location of NTM (red), EC deposition (green) and its FWHM (green shaded). c. The normalized misalignmer

$$\frac{\tau_R}{r_s}\frac{dW}{dt} = r_s\Delta'_0 + r_s\delta\Delta'_0 + a_2\frac{j_{bs}}{j_p}\frac{L_q}{W}\left[1 - \frac{W_{marg}^2}{3W^2}\right] - K_1\frac{j_{EC}}{j_{bs}} - \alpha_H F_H \frac{W}{W_{dep}}\frac{P_{EC}\eta_{EC}}{I_{EC}}$$

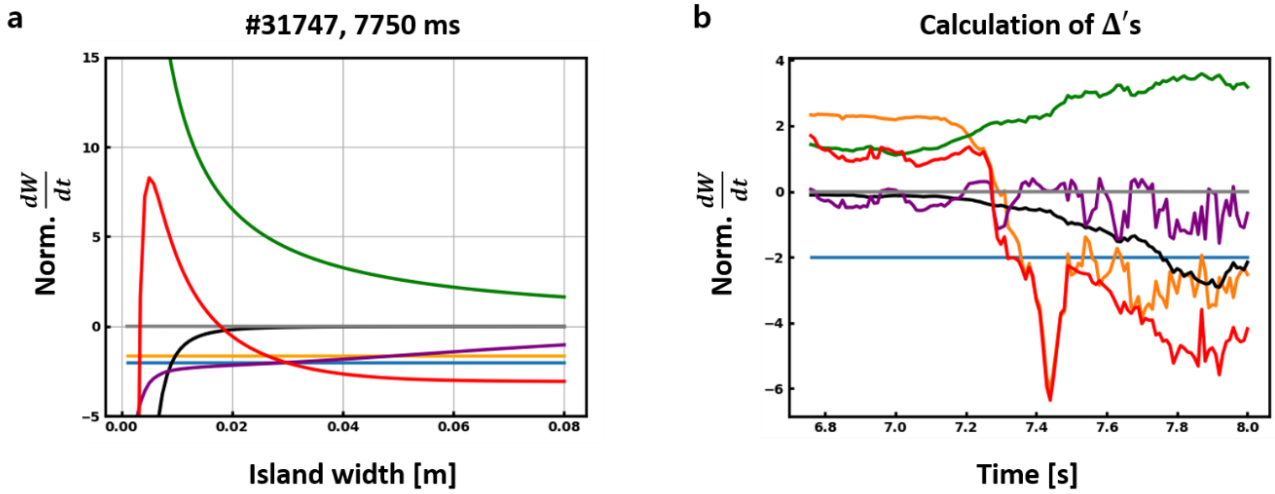

Fig. 6. MRE calculation result in KSTAR shot #31747. a. Along with island width. b. Along with time.

stopped fluctuating, the figure contains MRE terms from 6.75 s. After alignment from 7.3 s the EC related terms have negative values, implying their stabilizing effect. Therefore, we concluded that after the EC is aligned to the 2/1 NTM, it gradually stabilized NTM. In this experiment

4 Summary

In the NTM stabilization experiment with EC feedback control based on the minimum seeking method, we observed the gradual stabilization of the 2/1 NTM. Despite the minimum seeking controller initially failing to precisely find the NTM, the EC deposition became aligned with the NTM after 7.3 s. During this time range, the collective behaviour between the size of NTM and the plasma performance has ended. Therefore, the near stabilization is done after the alignment is fulfilled. Additionally, we observed the enhancement of plasma parameters such as the temperature, density, rotation, β_p, and more. Provided with the stability analyses with simplified MRE, we could find that the ECCD played a key role to stabilize the 2/1 NTM.

Nevertheless, there are rooms that the minimum seeking control can be done more appropriately. First, the controller needs a saturated NTM but if it fluctuates and the mode amplitude is influenced then the location of NTM can be misjudged as in this experiment. We can overcome this issue by generating saturated NTM or using real-time diagnose. Along with proper value of gain we can expect the more dynamic tracking in the precise control phase, and these are our next scope. Moreover, we can adjust the EC power modulation to inject EC in only the O-point, even if the ECCD deposited to the targeting rational surface properly. These approaches will enable us to address existing challenges more effectively and approach to stable operation of high-performance fusion plasmas by diminishing the deleterious NTMs.

This work was supported by the National R&D Program through the National Research Foundation of Korea (NRF) funded by the Korea government (Ministry of Science and ICT) (NRF-2021M1A7A4091135).

References

1. R. J. La Haye et al., Nucl. Fusion 37, 397 (1997) https://doi.org/10.1088/0029-5515/37/3/I08
2. Sauter et al., Phys. Plasmas 4, 1654 (1997) https://doi.org/10.1063/1.872270
3. R. Prater et al., Nucl. Fusion 47, 371 (2007) https://doi.org/10.1088/0029-5515/47/5/001
4. R. Prater, Phys. Plasmas 11, 2349 (2004) https://doi.org/10.1063/1.1690762
5. R. J. La Haye et al., Nucl. Fusion 48, 054004 (2008) https://doi.org/10.1088/0029-5515/48/5/054004
6. D. A. Humphreys et al., Phys. Plasmas 13, 056113 (2006) https://doi.org/10.1063/1.2173606
7. W. Wehner, E. Schuster, 18th IEEE Int. Conf. on Control Applications (Saint Petersburg, Russia, 8-10 July 2009) pp 853-60 (2009) https://doi.org/10.1109/CCA.2009.5280943
8. C. Zhang, R. Ordonez, Extremum-seeking control and applications: a numerical optimization-based

approach, (Springer Science & Business Media, 2011)
9. W. Wehner, E. Schuster, Nucl. Fusion **52**, 074003 (2012) https://doi.org/10.1088/0029-5515/52/7/074003
10. R. J. La Haye, Phys. Plasmas **13**, 055501 (2006) https://doi.org/10.1063/1.2180747
11. M. Maraschek et al., Phys. Rev. Lett. **98**, 025005 (2007) https://doi.org/10.1103/PhysRevLett.98.025005
12. B. A. Hennen et al., Plasma Phys. Control. Fusion **52**, 104006 (2010) https://doi.org/10.1088/0741-3335/52/10/104006
13. M. Lennholm et al., Nucl. Fusion **43**, 1458 (2003) https://doi.org/10.1088/0029-5515/43/11/019
14. F. Felici et al., Nucl. Fusion **52**, 074001 (2012) https://doi.org/10.1088/0029-5515/52/7/074001
15. K. Kim et al., Curr. Appl. Phys. **15**, 547–554 (2015) https://doi.org/10.1016/J.CAP.2015.01.032
16. A. Isayama et al., Nucl. Fusion **43**, 1272 (2003) https://doi.org/10.1088/0029-5515/43/10/031
17. M. Kim et al., Nucl. Fusion **55**, 023006 (2015) https://doi.org/10.1088/0029-5515/55/2/023006
18. M. Kim et al., Nucl. Fusion **56**, 038002 (2016) https://doi.org/10.1088/0029-5515/56/3/038002
19. M. Park et al., Nucl. Fusion **58**, 016042 (2017) https://doi.org/10.1088/1741-4326/aa95d1
20. H. P. Furth, J. Killeen, M. N. Rosenbluth, Phys. Fluids **6**, 459-484 (1963) https://doi.org/10.1063/1.1706761
21. R. J. Goldston, Introduction to Plasma Physics, (CRC Press, Boca Raton, 2020)
22. P. H. Rutherford, Phys. Fluids **16**, 1903 (1973) https://doi.org/10.1063/1.1694232
23. C. Y. Lee et al., Nucl. Fusion **61**, 096020 (2021) https://doi.org/10.1088/1741-4326/ac1690
24. K. Kim, L. Terzolo, Y. S. Na, 38th European Physical Society Conf. on Plasma Physics (Strasbourg, France, 27 June-1 July 2011) P2.086 (2011)
25. G. S. Yun et al., Rev. Sci. Instrum. **85**, 11D820 (2014) https://doi.org/10.1063/1.4890401
26. A. H. Kritz et al., in Proceedings of 3rd Int. Symp. Heating in Toroidal Plasmas ECE (Brussels, Belgium), pp. 707–723 (1982) https://doi.org/10.1016/B978-1-4832-8428-6.50081-3
27. L. L. Lao et al., Nucl. Fusion **25**, 1611 (1985) https://doi.org/10.1088/0029-5515/25/11/007
28. L. L. Lao et al., Fusion. Sci. Technol. **48**, 968-977 (2005) https://doi.org/10.13182/FST48-968
29. H. Lütjens et al., Comput. Phys. Commun. **97**, 219 (1996) https://doi.org/10.1016/0010-4655(96)00046-X
30. A. Pankin et al., Comput. Phys. Commun. 159, 157 (2004) https://doi.org/10.1016/j.cpc.2003.11.002
31. O. Sauter et al., Phys. Plasmas 6, 2834 (1999) https://doi.org/10.1063/1.873240